06

Sorption properties of a magnetically sensitive composite based on few-layer graphene towards methylene blue

© A.A. Vozniakovskii,[1] E.A. Bogacheva,[1] N.D. Podlozhnyuk,[1] A.P. Voznyakovskii,[2] S.V. Kidalov[1]

[1] Ioffe Institute,
194021 St. Petersburg, Russia
[2] Lebedev Institute of Synthetic Rubber,
198035 St. Petersburg, Russia
e-mail: alexey_inform@mail.ru

Received October 3, 2024
Revised October 3, 2024
Accepted October 3, 2024

A method for modifying few-layer graphene particles obtained under self-propagating high-temperature synthesis with magnetic particles by synthesizing magnetite by chemical condensation has been developed. The efficiency of such a composite as a sorbent for water purification from methylene blue was studied. It has been established that the obtained magnetic composite, although inferior in sorption efficiency to the original particles of few-layer graphene, is highly sensitive to the effects of an external magnetic field, which makes it easy to remove it from water along with the sorbed pollutant.

Keywords: few-layer graphene, magnetite, purification, sorption.

DOI: 10.61011/TP.2025.02.60820.281-24

Introduction

Graphene derivatives are known to have outstanding adsorptive properties with respect to organic dyes such as methylene blue [1], rhodamine G [2] that are discharged by cosmetic manufacturers and textile factories into waste water, various toxins [3] and viral infections [4]. Popularity of graphene nanostructures as sorbents is attributed to their properties: high specific surface area (to $2600\,m^2/g$) [5], and high content of oxygen-containing functional groups on the surface (to 30 mass%) [6].

However, despite a high potential of graphene nanostructures (GNS), they haven't been transferred into practice yet for a number of reasons. Due to the imperfection of GNS synthesis techniques, both using bottom-up and top-down approaches, large amounts of high quality GNS with reasonable cost cannot be achieved to date [7]. Moreover, as long as biosafety of GNS is still debatable, there is a problem of full GNS removal from the water volume after decontamination.

Due to the problem of graphene particle separation from an adsorbate solution, many researchers put a question of adsorbent particle separation from a pollutant solution to improve the adsorption and water treatment process efficiency. One of the methods used to solve this task is the synthesis of magnetic particles (shell) with graphene structures (nucleus) [8–13].

The key idea of this approach is in the increase of mixture separation efficiency due to magnetic separation. Several requirements are imposed to a composite material based on magnetic particles: particles shall have homogeneity, chemical stability, stability in water, as well as maintain magnetic properties in a medium where sorption will be performed in future. Studies [14] described the purpose of magnetic sorbents under a common name „ferrocarbon" for medical use. Porous microgranules $2-5\,\mu m$ in size with iron particle inclusions were made from carbon. Due to the inclusions, such sorbents lost their sorption capacity by approx. 5–7%, however, acquired mobility in magnetic field, which rendered a transportation function to these sorbents. Medical delivery to an affected area may be performed using a magnetic liquid drop, for example, biologically compatible magnetic water-based liquid with ascorbic acid as a stabilizer [15].

This work describes the study of methylene blue sorption properties of a magnetic composite material based on few-layer graphene (FLG) fabricated in the self-propagating high-temperature synthesis conditions from cellulose [16]. This technique makes it possible to produce large amounts of FLG free of the Stone-Wales defects [17], in the powder form. Previous studies established that FLG produced using this technique may be successfully used as a sorbent to remove industrial dyes from water [18].

1. Experimental

1.1. Feedstock

Initial FLG was prepared in the self-propagating high-temperature synthesis conditions from cellulose (AR grade,

India) and ammonia nitrate (AR grade, Russia) at the ratio of 3:7. The synthesis technique was detailed in [16].

The synthesis of a FLG-based magnetic composite material used iron (III) chloride hexahydrate and iron (II) sulfate heptahydrate (AR grade, Russia) and NH_4OH (AR grade, Russia). The synthesis also used deionized water ($0.5\,\mu$S/cm).

1.2. FLG-based magnetic composite material synthesis

The composite material sample was prepared in water medium using the ULAB overhead stirrer at 70°C. For this, 2 g of iron(III) chloride hexahydrate was dissolved in 20 ml of water, then 1 g of iron (II) sulfate heptahydrate and 1 g of FLG were added with vigorous stirring.

Magnetic composite material was formed in the ammonia medium (5 ml) where metal cations (shell) interacted electrostatically with FLG (nucleus) and agglomerated particles. For complete performance of the synthesis, the mixture was held for 5 min, then rinsed with water 5 times and separated using a magnet. Magnetic particle formation on the FLG surface takes place as follows

$$2FeCl_3 + FeSO_4 + 8NH_4OH + FLG \rightarrow FLG@Fe_3O_4 + 6NH_4Cl + (NH_4)2SO_4 + H_2O. \quad (1)$$

Theoretical product yield is equal to 2.63 g, and practical yield is 2.00 g, which is associated with incomplete reactivity of initial components and multiple rinsing of the obtained product. Mass fractions of components (FLG and Fe_3O_4) in the final composite material were 1 to 1.

1.3. Characterization of the synthesized FLG-based magnetic composite material

Surface morphology of the magnetic composite material was studied using the Mira-3M (TESCAN) scanning electron microscope. Sample preparation included application of the magnetic composite powder to the Mira-3M (TESCAN, Czech Republic) double-sided carbon conductive tape. IR spectra of the magnetic composite material were recorded using the Infralum FT-08 (Lumex-Marketing, Russia) spectrometer. Specific surface area of the sample was also measured with indication of pore volume by the BET low-temperature nitrogen sorption using the Sorbi-MS (Meta, Russia) meter.

1.4. Study of sorption properties of the FLG-based magnetic composite material

Adsorption activity of the composite material with respect to the organic dye, methylene blue, was studied depending on four conditions: adsorbent weight, time, sorption and medium acidity. Thus, the initial solution with dye concentration of 1 g/l provided solutions with the desired concentration by dilution of the initial solvent. Sorption was performed in 250 ml flat-bottom flask, dye solution volume was 100 ml. Adsorbent was added to a solution with known concentration and held in the specified conditions. Magnetic composite material was removed from the dye solution at the end the experiment using a magnet with precipitation on the flask bottom — the process took max. 20 s. Equilibrium concentration of the methylene blue solution was determined by the absorbance at a maximum wavelength of 660 nm using the UF-1800 ECOVIEW (Shanghai Mapada Instruments Co., Ltd., China) spectrophotometer. Specific sorption capacity q_e was calculated using equation (2):

$$q_e = \frac{C_0 - C_e}{m} V, \quad (2)$$

where C_0 is the pre-sorption concentration of methylene blue solution, [mg/l]; C_e is the post-sorption concentration of methylene blue solution, [mg/l]; m is the weight of magnetic composite material, [g]; V is the solution volume, [l].

The sorption time effect on the specific sorption capacity q_e was studied using the methylene blue solution, concentration 100 mg/l, volume 100 ml and sorbent weight equal to 50 mg. The solutions were held on the S-3.02 20M (ELMI, Latvia) autoshaker within the time range from 10 min to 180 min.

To study the sorption temperature effect, solutions were prepared within the concentration range from 10 mg/l to 200 mg/l, with volume 100 ml and sorbent weight equal to 50 mg at 20 and 60°C. The mixtures were held in a water thermostat during 3 h.

The medium acidity effect on the specific sorption capacity q_e was studied using the methylene blue solution, concentration 100 mg/l, volume 100 ml and sorbent weight equal to 50 mg. Medium acidity was adjusted by dropwise addition of 0.1 M NaOH and HCl solutions.

Sorption data is also analyzed by means of isothermal simulation. Correlation between the concentration of dye adsorbed by the adsorbent surface and the concentration of liquid-phase dye in equilibrium is evaluated by linearized Langmuir and Freundlich isotherms [19].

The Langmuir equation is used to evaluate the maximum adsorption capacity:

$$\frac{C_e}{q_e} = \frac{1}{K_L q_{\max}} + \frac{C_e}{q_{\max}}, \quad (3)$$

where q_e is the equilibrium adsorption capacity, [mg/l]; C_e is the equilibrium concentration of dye (methylene blue) in the solution, [mg/l]; $q_{\max}$ is the maximum adsorption capacity of adsorbent, [mg/l]; K_L is the Langmuir isotherm constant associated with the free adsorption energy.

The Freundlich isotherm is based on the multimolecular capability to adsorb organic molecules on heterogeneous solid surfaces. Linear form of Freundlich's equilibrium

Figure 1. Image of the FLG-based magnetic composite material exposed to a magnetic field.

adsorption equation is written as:

$$\ln q_e = \frac{1}{n} \ln C_e + \ln K_F, \qquad (4)$$

where q_e is the number of organic molecules adsorbed in equilibrium, [mg/l]; $1/n$ is the constant related to the adsorption intensity; C_e is the equilibrium concentration of organic molecules, [mg/l]; K_F is the Freundlich constant related to the maximum adsorption capacity or adsorbate.

2. Findings and discussion

Figure 1 shows the image of the FLG-based magnetic composite material exposed to a magnetic field.

As shown in the figure, the FLG-based magnetic composite material actively responds to the external magnetic field.

Characteristics of FLG sample surface

Sample	Specific surface area, m^2/g	Pore volume, cm^3/g
Initial FLG	661±17	0.397 ± 0.05
Magnetic composite material	403±10	0.341 ± 0.05

Note that the whole volume of FLG is successfully extracted using the external magnetic field, and no precipitation was observed in the solution which indicated a strong interaction between FLG particles and iron magnetic particles.

Figure 2 shows electron images of the initial FLG and FLG-based magnetic composite material. A FLG powder particle is an aggregate consisting of several smaller FLG slices. The magnetic composite material is in turn composed of the same FLG aggregates on the surface of which there are Fe_3O_4 clusters with various sizes.

Specific surface areas and pore volumes of the initial FLG and FLG-based magnetic composite material. The obtained results show that the specific surface area and porosity of the magnetic composite material are lower compared with the initial FLG, which may be associated with the fact that a part of the surface and pores are occupied by magnetosensitive iron particles.

Figure 3 shows the differential pore diameter distribution of the initial FLG and FLG-based magnetic composite material. The figure shows that the mean pore sizes of the magnetic composite material are larger than those of the initial FLG. Iron ion adsorption during the magnetic composite material synthesis presumably takes place primarily in pores with a diameter up to 25 nm.

Figure 4 shows IR spectra of the initial FLG and FLG-based magnetic composite material. A wide band at $630\,cm^{-1}$ may be assigned to the Fe−O vibrations in Fe_3O_4. Appearance of high-frequency bands in the magnetic composite material compared with the reference spectrum of Fe_3O_4 is explained by the presence and ordering of cation vacancies in the oxide structure.

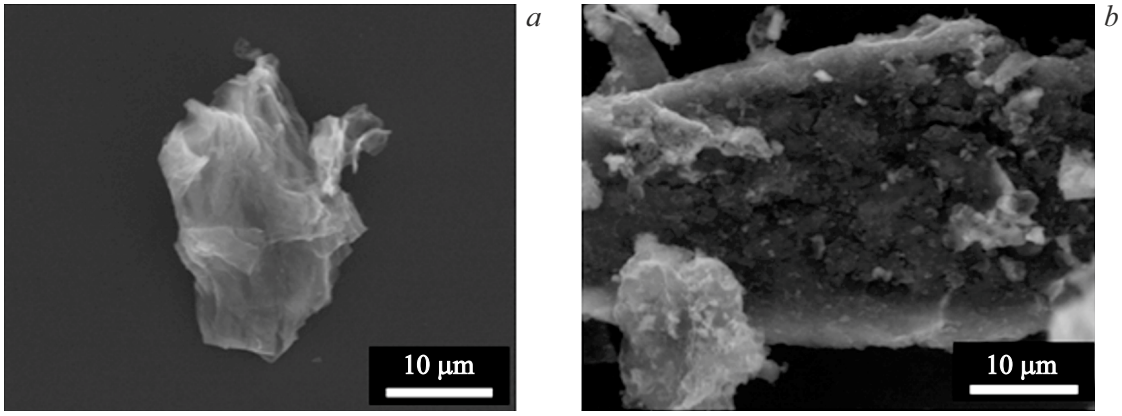

Figure 2. Electron images of the initial FLG (a) and FLG-based magnetic composite material (b).

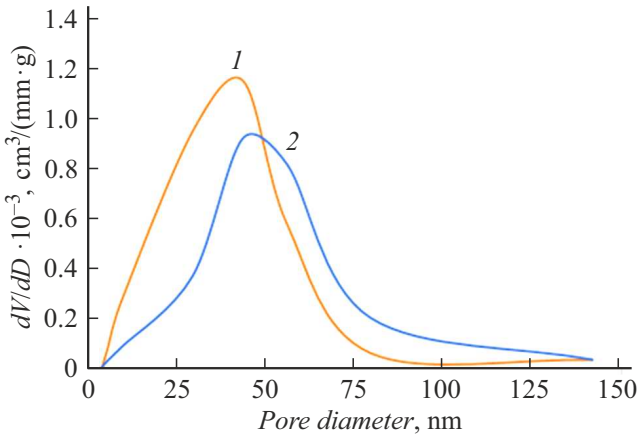

Figure 3. Differential pore diameter distribution: *1* — initial FLG; *2* — magnetic composite material.

Shift of peak 638–639 to 616 cm^{-1} may be caused by the change of iron ion environment symmetry resulting from phase transitions in the γ-Fe_2O_3 clusters in α-Fe_2O_3. The magnetic composite material also maintained the peaks at 3400 and 1600 cm^{-1}corresponding to stretching of hydrogen-related hydroxyl groups. There is also a peak on the magnetic composite material and FLG at 2225 cm^{-1} that defines the presence of nitrile group –CN, and a peak at 2974 cm^{-1} –C–H also appears.

Figure 5 shows the dependences of sorption capacity of the initial FLG and FLG-based magnetic composite material depending on the concentration of methylene blue. The results provided in the figure show that with the increase in the concentration of methylene blue, the magnetic composite material attains the saturation faster than the initial FLG because a part of the surface is occupied by magnetite particles, while the FLG keeps its sorption capacity in these conditions.

Figure 6 shows the dependences of sorption capacity of the initial FLG and FLG-based magnetic composite material on the concentration of methylene blue in the solution at various temperatures. The figure shows that, as the temperature increases from 20 to 60°C, the sorption capacity of the magnetic composite material increases by 60%, thus, the sorption process is endothermic.

Figure 7 shows the methylene blue adsorption on the magnetic composite material depending of the solution pH.

As shown in the figure, the solution acidity affects considerably the dye (methylene blue) absorption. Increase in pH from 2 to 11 leads to a maximum twofold

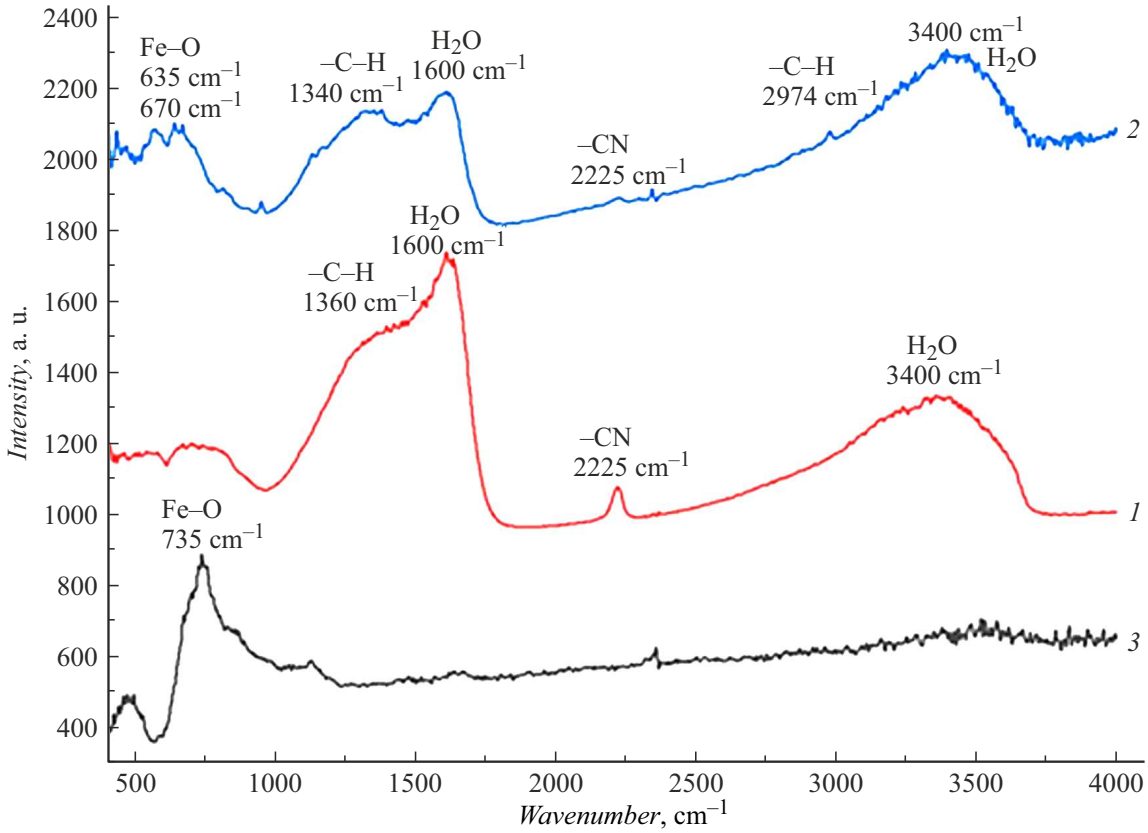

Figure 4. IR spectra: *1* — initial FLG, *2* — magnetic composite, *3* — Fe_3O_4.

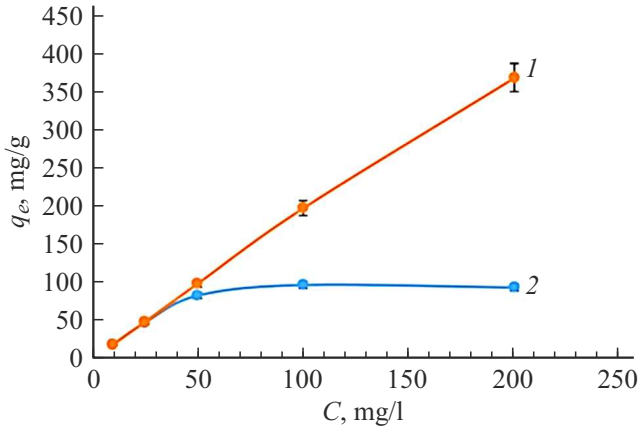

Figure 5. Dependence of the sorption capacity on the concentration of methylene blue in solution: *1* — initial FLG; *2* — magnetic composite material.

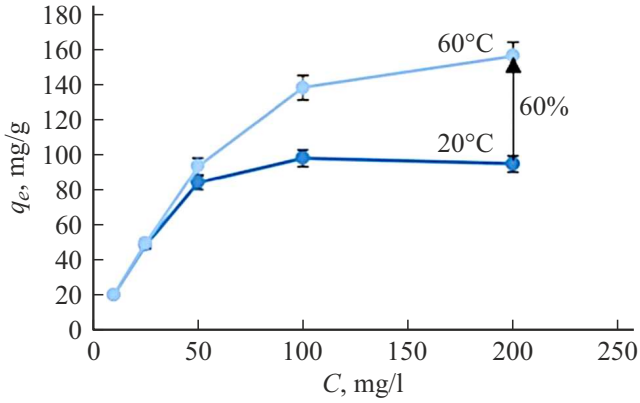

Figure 6. Dependence of sorption capacity of the initial FLG and FLG-based magnetic composite material on the concentration of methylene blue in the solution at various temperatures.

increase in the sorption capacity. Such difference is caused by the presence of oxygen-containing functional groups — carboxyl and hydroxyl groups on the FLG surface (Figure 4). This makes adsorption possible due to the electrostatic interaction, and these groups are ionized additionally as the solution pH increases, which additionally promotes adsorption according to this mechanism.

Figure 8 shows the sorption capacity measurements of the FLG-based magnetic composite material depending on the sorption time. The study of the sorption time effect on the sorption capacity of the prepared composite material showed that saturation occurs after approx. 90 min with the maximum value reached at approx. 110 mg/g.

Figure 9 shows the Langmuir and Freundlich sorption isotherms. Note that the Freundlich isotherm describes the sorption process in the best way (correlation coefficient

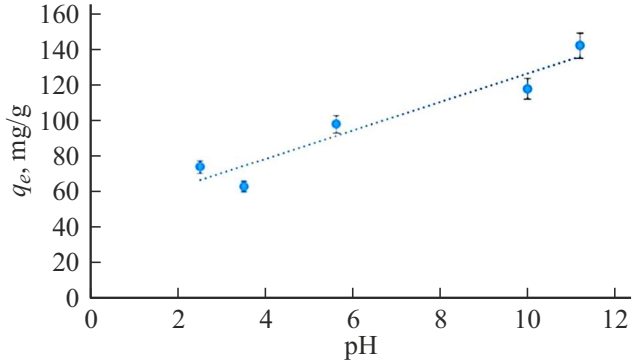

Figure 7. pH effect on the sorption capacity of magnetic composite material.

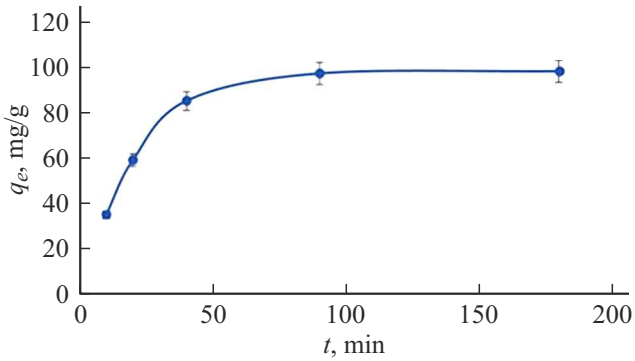

Figure 8. Sorption time effect on the sorption capacity of magnetic composite material.

0.971), which suggests a heterogeneous type of the sorbent surface.

Conclusion

The study showed that a FLG-based magnetic composite material may be synthesized in the self-propagating high-temperature synthesis conditions. Despite the fact that this magnetic composite material has a lower sorption efficiency with respect to methylene blue than the initial FLG, this composite material, due to its high sensitivity to external magnetic field, can be removed from a water volume much easier (during max. 20 s) using a magnet without any additional filtration. Further studies shall improve the ratio between FLG and magnetic iron particles to increase the sorption properties of the final composite material, and investigate the composite material efficiency with respect to other pollutants.

Funding

The study was carried out with financial support provided by the state assignment of the Ioffe Institute (FFUG-2024-0019 „Functional carbon nanostructured materials“).

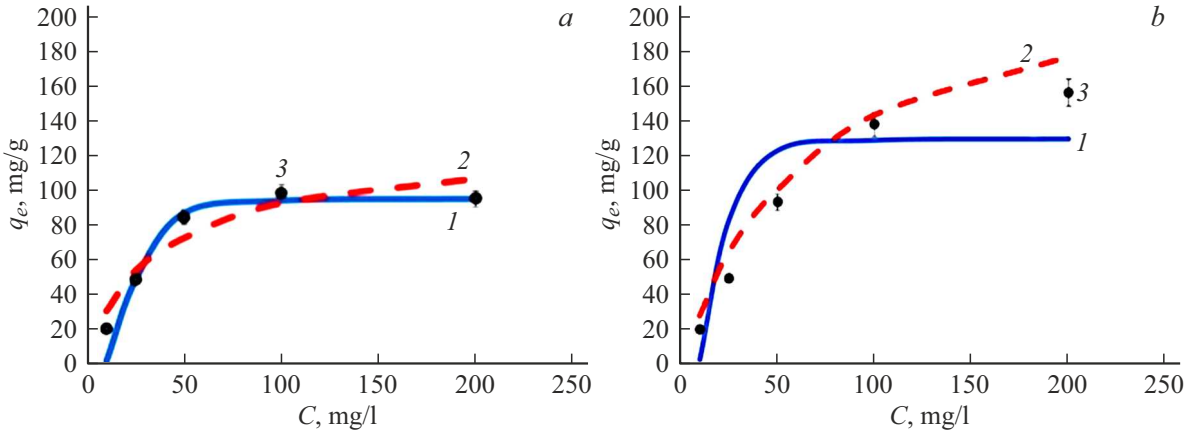

Figure 9. Langmuir and Freundlich sorption isotherms: *a* — 20, *b* — 60°C; *1* — Langmuir isotherm, *2* — Freundlich isotherm, *3* — experimental data.

Conflict of interest

The authors declare no conflict of interest.

References

[1] A. Arabpour, S. Dan, H. Hashemipour. Arabian J. Chem., **14** (3), 103003 (2021). DOI: 10.1016/j.arabjc.2021.103003

[2] K. Zhang, S. Yu, B. Jv, W. Zheng. Phys. Chem. Chem. Phys., **18** (41), 28418 (2016). DOI: 10.1039/C6CP03987A

[3] A.P. Voznyakovskii, A.P. Karmanov, L.S. Kocheva, A.Yu. Neverovskaya, A.A. Vozniakovskii, A.V. Kanarskii, E.I. Semenov, S.V. Kidalov. Tech. Phys., **68** (7), 132 (2023). DOI: 10.1134/S1063784223090165

[4] I.A. Eliseev, E.A. Gushchina, S.A. Klotchenko, A.A. Lebedev, N.M. Lebedeva, S.P. Lebedev, A.V. Nashchekin, V.N. Petrov, M.V. Puzyk, A.D. Roenkov, A.N. Smirnov, E.M. Tanklevskaya, A.S. Usikov, E.I. Shabunina, N.M. Schmidt. Tech. Phys., **57** (12), 524 (2022). DOI: 10.1134/S1063782623080031

[5] Y. Zhu, S. Murali, W. Cai, X. Li, J.W. Suk, J.R. Potts, R.S. Ruoff. Adv. Mater., **22** (35), 3906 (2010). DOI: 10.1002/adma.201001068

[6] V.N. Postnov, O.V. Rodinkov, L.N. Moskvin, A.G. Novikov, A.S. Bugaichenko, O.A. Krokhina. Russ. Chem. Rev., **85** (2), 115 (2016). DOI: 10.1070/RCR4551

[7] X. Gu, Y. Zhao, K. Sun, C.L. Vieira, Z. Jia, C. Cui, Z. Wang, A. Walsh, S. Huang. Ultrason. Sonochem., **58**, 104630 (2019). DOI: 10.1016/j.ultsonch.2019.104630

[8] A. Mahrouz, S. Farzaneh. Microchim. Acta, **183**, 1749 (2016). DOI: 10.1007/s00604-016-1805-8

[9] W. Tieshi, L. Zhaohong, L. Mingming, W. Bo, O.J. Qiuyun. Appl. Phys., **8**, 024314 (2013). DOI: 10.1063/1.4774243

[10] Y. Yunjin, M. Shiding, L. Shizhen, M. Li Ping, S. Hongqi, W. Shaobin. Chem. Eng. J., **184**, 326 (2012). DOI: 10.1016/j.cej.2011.12.017

[11] K. Rakesh, B. Sayan, S.J. Prabhakar. Environ. Chem. Eng., **9** (5), 16 (2021). DOI: 10.1016/j.jece.2021.106212

[12] S. Xiaosan, Z. Jie, F. Jishuo, Z. Qianqian, W. Sanfan. Mater. Res. Express, **9** (2), 020002 (2022). DOI: 10.1088/2053-1591/ac52c6

[13] T.V. Bukreeva, O.A. Orlova, S.N. Sulyanov, Y.V. Grigoriev, P.V. Dorovatovskiy. Crystall. Rep., **56** (5), 880 (2011). DOI: 10.1134/S1063774511050051

[14] L.Kh. Komissarova, V.I. Filippov. J. Magn. Magn. Mater., **225**, 197 (2001). DOI: 10.1016/S0304-8853(00)01258-0

[15] G.G. Tatishvili, M.G. Akhalaya, Z.A. Zurabashvili. Vestnik khirurgii, **4**, 37 (1989) (in Russian).

[16] A.P. Voznyakovskii, A.A. Vozniakovskii, S.V. Kidalov. Nanomater., **12** (4), 657 (2022). DOI: 10.3390/nano12040657

[17] A.P. Voznyakovskii, A.Yu. Neverovskaya, A.A. Vozniakovskii, S.V. Kidalov. Nanomater., **12** (5), 883 (2022). DOI: 10.3390/nano12050883

[18] N.D. Podlozhnyuk, A.A. Vozniakovskii, A.P. Voznyakovskii, S.V. Kidalov, E.A. Bogacheva. Russ J. Appl. Chem., **96** (2), 198 (2023). DOI: 10.1134/S1070427223020107

[19] J. Nusrat, R. Hridoy, H. Akter. Case Stud. Chem. Environ. Eng., **6** (10), 100239 (2022). DOI: 10.1016/j.cscee.2022.100239

Translated by E.Ilinskaya